HHS Public Access

Author manuscript

Bioconjug Chem. Author manuscript; available in PMC 2018 April 30.

Published in final edited form as:

Bioconjug Chem. 2018 April 18; 29(4): 1047–1059. doi:10.1021/acs.bioconjchem.7b00714.

New Mechanism for Release of Endosomal Contents: Osmotic Lysis via Nigericin-Mediated K^+/H^+ Exchange

Loganathan Rangasamy[†], **Venkatesh Chelvam**[†,‡], **Ananda Kumar Kanduluru**[†], **Madduri Srinivasarao**[†], **N. Achini Bandara**[†], **Fei You**[§], **Esteban A. Orellana**[||], **Andrea L. Kasinski**[||], and **Philip S. Low**[*,†]

[†]Purdue Institute for Drug Discovery, 720 Clinic Drive, West Lafayette Indiana 47907, United States

[‡]Discipline of Chemistry, Centre for Biosciences and Biomedical Engineering, Indian Institute of Technology, Indore, Madhya Pradesh, 453552, India

[§]Endocyte, Inc., 3000 Kent Avenue, Suite A1-100, West Lafayette, Indiana 47906, United States

[||]Department of Biological Sciences, Bindley Bioscience Center, Purdue University, West Lafayette, Indiana 47907, United States

Abstract

Although peptides, antibodies/antibody fragments, siRNAs, antisense DNAs, enzymes, and aptamers are all under development as possible therapeutic agents, the breadth of their applications has been severely compromised by their inability to reach intracellular targets. Thus, while macromolecules can often enter cells by receptor-mediated endocytosis, their missions frequently fail due to an inability to escape their entrapping endosomes. In this paper, we describe a general method for promoting release of any biologic material from any entrapping endosome. The strategy relies on the fact that all nascent endosomes contain extracellular (Na^+-enriched) medium, but are surrounded by intracellular (K^+-enriched) fluid in the cytoplasm. Osmotic swelling and rupture of endosomes will therefore be facilitated if the flow of K^+ down its concentration gradient from the cytosol into the endosome can be facilitated without allowing downhill flow of Na^+ from the endosome into the cytosol. While any K^+ selective ionophore can promote the K^+ specific influx, the ideal K^+ ionophore will also exchange influxed K^+ for an osmotically inactive proton (H^+) in order to prevent buildup of an electrical potential that would rapidly halt K^+ influx. The only ionophore that catalyzes this exchange of K^+ for H^+ efficiently is nigericin. We demonstrate here that ligand-targeted delivery of nigericin into endosomes that contain an otherwise impermeable fluorescent dye can augment release of the dye into the cell cytosol via swelling/bursting of the entrapping endosomes. We further show that nigericin-facilitated escape of a folate-

[*]Corresponding Author: plow@purdue.edu. Phone: 765-494-5272. Fax: 765-494-0239.

ORCID

Ananda Kumar Kanduluru: 0000-0003-2669-8665

Philip S. Low: 0000-0001-9042-5528

Supporting Information

The Supporting Information is available free of charge on the ACS Publications website at DOI: 10.1021/acs.bioconjchem.7b00714.

Additional details of experimental procedures including synthesis and characterization data of synthesized compounds (PDF)

The authors declare no competing financial interest.

targeted luciferase siRNA conjugate from its entrapping endosomes promotes rapid suppression of the intended luciferase reporter gene. Taken together, we propose that ionophore-catalyzed entry of K^+ into endosomal compartments can promote the release of otherwise impermeable contents from their encapsulating endosomes.

Graphical Abstract

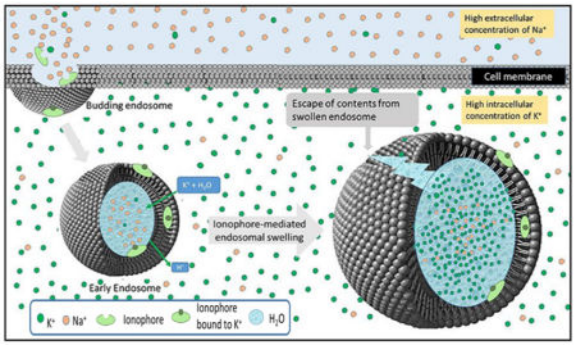

INTRODUCTION

Although the majority of prescription drugs today are small organic molecules, their share of the pharmaceutical market is declining in favor of biological macromolecules which now comprise ~39% of drugs in the pharmaceutical pipeline.[1] This shift toward biologics has been driven by both the diversity of biologic molecules that can be exploited for pharmacologic applications (e.g., oligonucleotides,[2] genes,[3] proteins,[4,5] peptides,[6] carbohydrates,[7,8] immune conjugates,[9–11] synthetic biopolymers,[12] etc.) and the increased numbers of diseases for which biologic therapies seem well suited.[13–17] Unfortunately, a major constraint still limiting the use of biologics is their inability to cross membranes, thereby confining their sites of action largely to extracellular spaces. Thus, the predominant targets of biologics today still constitute cell surface antigens,[18] secreted cytokines,[18] transmembrane receptors,[19] cell adhesion molecules,[20] and extracellular matrix proteins;[21,22] i.e., leaving the desirable intracellular signaling complexes, transcription factors, enzymatic pathways, structural assemblies, coding and non-coding RNAs, and chromatin remodeling components largely unaddressed.[23]

Although membrane barriers that restrict most biologics to extracellular spaces may differ somewhat among classes of macromolecular drugs, the most commonly encountered barrier lies in crossing the endosomal membrane. Thus, with the aid of a receptor-binding ligand, most macromolecules can be delivered via receptor-mediated endocytosis into an intracellular compartment. However, escape from that intracellular compartment into the cytoplasm is usually a low probability event. For example, during pinocytosis extracellular solutes can become entrapped within tiny (100 nm diameter) membrane invaginations that pinch off and traffic through intracellular endosomes; however, the internalized macromolecules rarely escape their entrapping compartments at any site along this pathway.[24] Similarly, during macropinocytosis much larger quantities of extracellular medium can become engulfed by a different internalization mechanism,[25] but again release of the

encapsulated macromolecules into the cytoplasm is very inefficient. While receptor-mediated endocytosis concentrates bound ligands (and any attached cargoes) onto cell surface receptors before transporting them into cells via membrane invagination,[26,27] the intracellular fates of such internalized biologics is again essentially the same, i.e., stable entrapment within an endosome.[23] Thus, regardless of the internalization pathway, escape of biologics from their encapsulating endosomes constitutes a limiting step in use of biologics to treat diseases originating within a cell.[23]

Because endosomal release has long been recognized as the primary barrier to broader use of biologic therapeutics, considerable effort has been devoted to finding strategies for release of biologic components. While most of such strategies show some degree of success *in vitro*, all have limitations that prevent their translation into clinical practice.[28] For example, cationic lipids and peptides are not only often toxic, but they may also bind nonspecifically to cell surfaces, thereby compromising potential applications in targeted drug delivery.[29] While "proton sponges" can induce counterion uptake and the consequent osmotic swelling of entrapping endosomes, they are also frequently toxic and the amount of material required to promote endosome lysis can also be clinically impractical.[30] And although pore-forming peptides can mediate escape of small molecules from intracellular compartments, their small pore sizes almost invariably prevent their use for delivery of larger biologics.[28] Finally, despite the established ability of certain photoactivatable dyes to induce endosomal lysis, use of such photolytic agents requires illumination of the targeted cell with a light source, greatly restricting its applicability to tissues that can be irradiated with light.[31–33] Taken together, an efficient method for facilitating release of biologics from entrapping endosomes is still lacking, and any new approach that might improve biologic delivery justifies further scrutiny. The strategy below has the potential to achieve this objective.

Summary of Strategy

In theory, any mechanism that can enhance the unidirectional entry of an osmotic solute into an endosome must promote the osmotic swelling of that endosome. In considering possible strategies that might induce this unidirectional flux of ions into an endosome, we realized that the endocytic process actually establishes the osmotic conditions that can facilitate such influx. Thus, any mammalian plasma membrane that invaginates and pinches off inside a cell will entrap a Na^+ rich extracellular fluid within the endosome and exclude a K^+ rich intracellular fluid that comprises the cytosol (Figure 1), i.e., setting up both K^+ and Na^+ gradients across the endosomal membrane.[34,35] Thus, any ionophore that can selectively transport K^+ down its concentration gradient (i.e., into the endosome) without simultaneously allowing Na^+ to flow down its concentration gradient out of the endosome must increase the osmotic pressure within the endosome. As diagrammed in Figure 1, such an increase in osmotic pressure within the endosome must force an influx of water that will swell the endosome. Moreover, analysis of the Nernst equation reveals that this endosome swelling will continue until either (i) the endosome bursts due to the rising osmotic pressure, or (ii) the rising electrochemical potential of K^+ across the endosomal membrane (i.e., due to buildup of intraluminal K^+ and its positive charge) reaches equilibrium, i.e., preventing further influx of K^+. Therefore, in order to enable K^+ to continuously enter the endosome unimpeded by a rising electrical potential, it seemed prudent to find a way to allow a

positive charge to leave the endosome without pulling any water with it. Since the only positively charged particle that is not osmotically active is the proton (H^+), this additional condition requires that we employ an ionophore that will exchange K^+ (but not Na^+) for H^+ (but not any other cation). Fortunately, nature has provided such an ionophore in the form of nigericin **1** (Figure 2A), which facilitates the electroneutral entry of an osmotically active K^+ in exchange for an osmotically inactive H^+, thereby promoting the osmotic swelling of an endosome unhindered by any buildup of membrane potential.[36]

In this paper we describe the use of nigericin to promote the osmotic lysis of endosomes and the consequent release of otherwise membrane-impermeable biologics from their entrapping intracellular compartments. We first show that a folate-rhodamine conjugate containing a membrane-impermeable rhodamine dye can enter endosomes via folate receptor-mediated endocytosis and be released from otherwise impermeable endosomes upon nigericin-mediated endosome swelling and bursting. We then demonstrate that siRNA-mediated knockdown of a luciferase reporter gene can be significantly enhanced when nigericin is codelivered with the folate-targeted siRNA. Taken together with the fact that nigericin is nontoxic to cells up to concentrations >100 nM (Figures S1B and S2),[37,38] these data suggest that nigericin-mediated swelling of endosomal compartments can facilitate release of biologics from entrapping endosomes without causing significant toxicity to the targeted cell.

RESULTS

To conduct an initial test of the concept proposed in Figure 1, we first investigated whether nigericin **1** (Figure 2A) could promote osmotic bursting of unilamellar calcein-containing liposomes that had been assembled with high intraluminal Na^+ and high extraluminal K^+, i.e., similar to the ion gradients surrounding endosomes in living cells. For this and subsequent purposes, we prepared the folatenigericin conjugate **2** (Figure 2A) by esterification of nigericin's free carboxylic acid to a hydrophilic peptide spacer that was in turn conjugated to folic acid for use in targeting folate receptor (FR) expressing cells. Because endosomal compartments are reducing in nature,[39] the design of the folate nigericin conjugate included a self-immolative disulfide linker[40] that is rapidly cleaved upon disulfide reduction, thereby releasing free nigericin into the entrapping endosome. As seen in Figure 2B, escape of the membrane-impermeable dye, calcein, from the synthetic unilamellar liposomes was maximal when the vesicles were quantitatively lysed with detergent (Triton X-100) (positive control). In contrast, release of the impermeable calcein was minimal when only buffer plus DMSO were added (negative control). Importantly, when the vesicle suspension was exposed to either free nigericin **1** or folate-nigericin conjugate (ester **2**, 100 nM) in the presence of 20 mM dithiothreitol (to promote disulfide bond reduction and nigericin release), nearly maximal escape of calcein was again observed (Figure 2B). Evidence that this calcein release was dependent on a Na^+/K^+ gradient across the liposomal membrane was established by demonstrating a lack of calcein release when the intraliposomal Na^+ was exchanged for the same concentration of liposomal K^+ (i.e., the electrochemical gradient was collapsed). Taken together, these data demonstrate that nigericin can mediate the bursting of a membrane-encapsulating compartment if the

compartment is constructed with a Na^+/K^+ transmembrane gradient similar to that seen in endosomes.

To determine whether nigericin might promote similar bursting of intracellular endosomes in living cells, we next treated FR-positive KB cells with a folate-rhodamine conjugate **4** (Figure 3A) that readily enters FR-expressing cells via folate receptor-mediated endocytosis.[39] Although the folate-rhodamine conjugate was designed to release free rhodamine following its endocytosis (due to reduction of its disulfide bond in intracellular endosomes),[39] the discharged rhodamine is known to remain entrapped within the endosome due to its strong positive and negative charges.[41] To evaluate whether nigericin might enable release of this entrapped rhodamine, 10 nM folate-rhodamine was added to FR-positive KB cells, in both the presence and absence of 100 nM folate-nigericin ester **2**. Because many FR are known to internalize into the same FR-positive endosome,[42] it was anticipated that multiple copies of both conjugates **2** and **4** would be internalized into each endosome, allowing the released nigericin to catalyze the escape of the rhodamine entrapped within the same endosome.

As shown in Figure 3B, the aforementioned predictions were only partially realized. As anticipated, within 1 h of conjugate **2** addition, rhodamine containing endosomes were seen to swell only in those cells treated with both folate-rhodamine plus folate-nigericin **2**, but not in cells treated solely with folate-rhodamine. These data suggested that folate-nigericin **2** was indeed required for endosome swelling. By 2 h post-administration, however, many of the nigericin-containing endosomes had continued to enlarge, expanding eventually to many times the size of folate-rhodamine containing endosomes in cells not treated with folate-nigericin, but surprisingly without bursting. Indeed, only a fraction of the swollen endosomes displayed plumes of escaping free rhodamine emerging from their surfaces (see green arrow, Figure 3B). Although by 3 h post-administration a greater fraction of the swollen endosomes showed plumes of released rhodamine (along with diffuse rhodamine staining within the cytoplasm), the majority of rhodamine fluorescence appeared to remain encapsulated within the greatly enlarged endosomes. Because endosomes in cells treated solely with folate-rhodamine **4** remained relatively unchanged except for the slow migration of the fluorescent endosomes toward the cell's interior, we conclude that enlargement and periodic rupture of endosomes requires the involvement of folate-nigericin. Whether the unanticipated continual endosome expansion occurs because the initial endosomes are part of an elaborate anastomosing network of intracellular compartments that share a common encapsulating membrane, or because the swelling endosomes are induced to rapidly fuse to increase their surface to volume ratios cannot be ascertained from the data. However, the fact that some release of contents occurs during swelling motivated us to explore this endosome escape strategy further.

To determine whether nigericin-mediated endosome swelling might be exploited to deliver a larger folate-targeted biologic into a cell's cytosol, we next constructed the folate-siRNA conjugate **5** shown in Figure 4A, where the targeting ligand (folate) was conjugated to the 3' end of one strand of a duplex siRNA, while a fluorescent dye (Dylight 647; (Dy647)) was linked to the 3' end of the complementary strand (Figure 4A). Based on this design, Dylight 647 binding and endocytosis should only be seen in fluorescence micrographs of treated

cells when the intact siRNA duplex is delivered into the cell. As shown in Figure 4B, few differences can be observed between folate-nigericin **2** treated and untreated cells during the first 3 h of incubation. However, by 5 h post-administration, significant swelling, aggregation, and pluming of fluorescence can be seen from endosomes in the folate-nigericin **2** treated samples, but not in control cells. Although these data suggest that endosome swelling and leakage may require more time to release the larger folate-siRNA conjugate, the end result appears to be the same, with endosome swelling and release of Dy647-siRNA (see green arrows in Figure 4B) also occurring when the biologic is larger.

Although nigericin is not highly toxic to mammals (LD_{50} in mice is only 190 mg/kg),[43] it was still important to minimize any premature release of ionophore that might occur during transit within the bloodstream to the target cell. For this purpose, we explored whether a more stable carbamate linkage to nigericin (Figure 5A, conjugate **6**) might prove equally potent in promoting endosome swelling. As shown in Figure 5B, endosome swelling and release was equally effective with the carbamate conjugate **6** as with the ester conjugate **2** (100 nM). Thus, not only was significant endosome enlargement/aggregation also apparent, but the usual plumes of released dye could even be seen inside the cells as early as 1 h after exposure (Figure 5B). These data suggest that use of the more stable carbamate linker does not compromise nigericin's ability to promote endosome bursting.

To further minimize any possible nigericin-mediated toxicity, we next explored whether lower concentrations of folate-nigericin might induce similar endosome swelling and rupture. As shown in Figure 6A, 60 nM folate-nigericin carbamate conjugate **6** still promoted endosome enlargement and rhodamine release (see Figure 5B). Curiously, 30 nM folate-nigericin carbamate conjugate **6** was also effective at inducing endosome enlargement and rhodamine release (Figure 6B). In contrast, still lower concentrations of folate-nigericin showed increasingly weaker potency (data not shown), suggesting that concentrations of targeted nigericin below 30 nM might not be adequate for catalysis of endosome swelling and rupture.

To explore the generality of nigericin-mediated endosome swelling, we elected to examine whether folate-targeted nigericin might facilitate endosome enlargement and leakage in two other unrelated cell types. First, since all of the above experiments were conducted on a nasopharyngeal cancer cell line (KB cells), we next conducted analogous studies on a triple negative breast cancer cell line (MDA-MB-231). As shown in Figure 7A, endosomal escape was again only observed in cells treated with a folate-nigericin conjugate, with pluming of rhodamine fluorescence appearing more frequently in cultures treated with the folate-nigericin amide than its ester counterpart. In fact, except for a somewhat delayed progression of the swelling/bursting process in MDA-MB-231 cells, the response of the cells to codelivery of nigericin was similar to that seen in KB cells.

Next, to explore whether a still more unrelated cell type might display a similar response to cointernalization of nigericin, we again conducted identical studies on RAW 264.7 cells, a malignant macrophage cell line that differs from KB cells not only in its cell of origin, but also in its targeted receptor (i.e., RAW264.7 cells express the beta form of the folate receptor rather than the alpha isoform present on KB and MDA-MB-231 cells).[44] As displayed in

Figure 7B, codelivery of nigericin into RAW264.7 endosomes promoted both endosome swelling and rhodamine release in a similar but less prominent manner than seen in KB cells. And again, these perturbations were completely absent in cells not treated with folate-nigericin ester conjugate **2**.

Finally, to confirm that the apparent nigericin-mediated swelling and leakage of endosomal contents can deliver a functional biologic into a target cell, the ability of a folate-conjugated antisense oligonucleotide (siLuc2) to suppress luciferase 2 gene expression was examined. For this purpose, MDA-MB-231 cells were stably transfected to constitutively express luciferase 2 and then incubated with a folate-siLuc2 antisense conjugate either lacking (**structure 7**) or containing at attached nigericin (**structure 8**). As shown in Figure 8C, no difference in luciferase activity could be detected between the two constructs for the first 18 h of incubation (perhaps due to the large number of pre-existing copies of luciferase enzyme in the cells). However, at later time points a significant difference in luciferase activity was observed, with little reduction seen in cultures exposed to the folate-siRNA lacking nigericin, but a significant decrease seen in cultures treated with the conjugate containing nigericin (see Figure S14 in Supporting Information for more controls). The reduced potency of luciferase gene suppression by the construct lacking nigericin strongly argues that endosome swelling and leakage can be facilitated by codelivery of nigericin into the endosomes.

DISCUSSION

The folate receptor is a membrane-anchored protein that is rarely expressed on healthy cells[29] but overexpressed on ~40% of human cancer cells, including malignant cells from lung, breast, ovarian, colon, and kidney cancers.[45–48] Not surprisingly, FRα has been frequently exploited for receptor-mediated delivery of folate-linked membrane-permeable drugs into cancer cells,[47,49–52] since escape of membrane-permeable drugs from entrapping endosomes proceeds by passive diffusion. In contrast, the ability of membrane-impermeable drugs to escape entrapping endosomes has been disappointing to date,[53] with most biologic drugs never accessing their targets in the cytoplasm. Because nearly all receptor-mediated delivery pathways suffer from this same limitation, targeted delivery of biologics into pathologic cells will not likely be possible until a clinically useful endosome escape mechanism can be developed. To test the ability of nigericin to mediate osmotic lysis of endosomes, we constructed multiple membrane-impermeable folate conjugates that could only enter a cell's cytosol if its internalizing endosomes were ruptured. Using this system we were able to demonstrate that ester-, amide-, and carbamate-bridged folate-nigericin conjugates could all successfully promote release of otherwise impermeable folate-rhodamine and folate-siRNA conjugates from intracellular endosomes in KB, MDA-MB-231, and RAW274.7 cells. Taken together, we conclude that codelivery of nigericin into entrapping endosomes can mediate osmotic swelling and at least partial lysis of endosomes, allowing escape of entrapped contents into a target cell's cytoplasm.

Why might a nigericin-mediated endosome lysis strategy be preferred over other endosome release mechanisms? From our perspective, use of nigericin may primarily be favored because of its ease of translation into the clinic. Thus, nigericin is a small, stable, well-

characterized, nontoxic, and easily conjugatable organic molecule that can be attached via a variety of self-immolative linkers to virtually any biologic molecule destined for clinical use. Because the resulting conjugate can be prepared in a homogeneous formulation that can be molecularly characterized by FDA-approved methods,[54] its stability and manufacturing reproducibility should be readily documentable. Moreover, by avoiding problems with toxicity, homogeneity, and efficacy that can plague cell permeating peptides, polycations, pore-forming peptides, and proton sponges, many of the pitfalls that limit utility of other endosome escape mechanisms can be circumvented. It is our hope that with further refinement and optimization, incorporation of one or more nigericins (or a related ionophore) into biologic drugs will eventually enable their use in the treatment of diseases that are driven by intracellular targets.

MATERIALS AND METHODS

Preparation of Calcein Loaded Unilamellar Liposomes

20 mg of L-α-phosphatidylcholine (from egg), 8 mg of cholesterol, and 2 mg of phosphatidylglycerol were dissolved in 2 mL of chloroform/methanol (2:1 v/v) in a 50 mL round-bottom flask by slightly warming the contents (40–50 °C) until the lipids were miscible in the solvent. The solvent was then evaporated on a rotary evaporator under low pressure until a thin film of lipid was deposited on the walls of the flask. The residual solvent was evaporated under high vacuum for 1 h and 1 mL of 130 mM NaCl/20 mM Na_3PO_4 buffer (adjusted to pH 7 with HCl) containing 50 mM calcein dye (Sigma-Aldrich) was added to the flask. The lipid film was disrupted by stirring with magnetic glass beads at room temperature to yield a milky suspension of liposomes. Liposomes were then sonicated under N_2 for 10 min to prepare unilamellar liposomes. These liposomes were transferred to a high potassium buffer by passing through a PD MidiTrap G-25 column using an eluent mixture of 130 mM KCl and 20 mM K_3PO_4 buffer (adjusted to pH 7 with HCl). Liposomes were refrigerated (0–4 °C) until use.

Characterization of the Liposomes

The liposome size and zeta-potential were measured using dynamic light scattering (Zetasizer Nano ZS, Malvern). Measurements were performed by dispersing liposomes in buffer (1:500) (130 mM KCl/20 mM K_3PO_4 buffer, pH 7.6). The temperature was set at 25 °C for all measurements. Three measurements were made per sample, and the averaged data was reported. The size of the liposomes were in the range of 400 ± 15 nm and charge of the liposome were −49.0 ± 1.6 mV

Cryo-TEM Measurement

The liposomes were applied to lacey carbon grids (Ultrathin Carbon Film on a Lacey Carbon Support Film, 01824, Ted Pella) in 3 μL volume under ~90% relative humidity and double-blotted for 6 s. The liposome sample was flash frozen in liquid ethane using the semiautomated plunger Cp3 (Gatan). The flash-frozen sample was loaded on a CM200 transmission electron microscope under liquid nitrogen cryogenic conditions. The sample was screened at a nominal magnification of 50,000× for the presence of liposomes.

Micrographs were binned twice using ImageJ to better visualize liposomes (see Supporting Information, Figure S15).

Assay of Calcein Release from Liposomes

10 μL of liposomes suspended in 1 mL of the 130 mM KCl and 20 mM K_3PO_4 buffer described above were placed in a transparent cuvette, with the addition of nigericin free acid or folate-nigericin conjugates at 100 nM in the presence of 20 mM DTT. The intensity of the absorption maximum was measured using a fluorescence spectrophotometer. Figure 2 presents a comparison of calcein dye release by various treatments of liposomes, including controls.

Relative Affinity Assay

FR-positive KB cells were gently trypsinized in 0.25% trypsin in phosphate-buffered saline (PBS) at room temperature and then diluted in folate-deficient RPMI medium (FDRPMI) containing 10% heat-inactivated fetal calf serum. After a 5 min 800*g* spin and one PBS wash, the final cell pellet was suspended in FDRPMI 1640 (no serum). Cells were incubated for 15 min on ice with 100 nmol/L of 3H-folic acid in the absence and presence of increasing concentrations of folate-nigericin. Samples were centrifuged at 10,000*g* for 5 min; cell pellets were suspended in buffer, transferred to individual vials containing 5 mL of scintillation cocktail, and then counted for radioactivity. Negative control tubes contained only the 3H-folic acid in FDRPMI (no competitor). Positive control tubes contained a final concentration of 1 mmol/L folic acid, and disintegrations per minute (dpm) measured in these samples (representing nonspecific binding of label) were subtracted from all samples. Notably, relative affinities were defined as the inverse molar ratio of compound required to displace 50% of 3H-folic acid bound to the FR on KB cells, and the relative affinity of folic acidfor the FR was set to 1.

Determination of Nigericin Toxicity (IC_{50})

KB cells (100,000 cells/well) were seeded on amine-coated 24-well plates and allowed to form monolayers. After allowing the cells to reach ~60% confluence, spent medium was replaced with fresh medium and the desired concentrations of nigericin were added to each well. After incubating for 2 h at 37 °C, cells were rinsed 3× with fresh medium and then incubated an additional 66 h at 37 °C in fresh medium. Spent medium in each well was again replaced with fresh medium (0.5 mL) containing ^{3}H-thymidine (1 μCi/mL), and the cells were incubated for an additional 4 h. After washing the cells 3× with medium, they were dissolved in 0.5 mL of 0.25 M NaOH. Thymidine incorporation was then determined by counting cell-associated radioactivity using a scintillation counter (Packard, Packard Instrument Company). The IC_{50} value was derived from a plot of the percent of ^{3}H-thymidine incorporation versus log concentration using Graph Pad Prism 4 and TableCurve 2D software.

Live Cell Proliferation Assay

KB cells were seeded in 96-well plates (Corning 3603; 2000 cells/well) and incubated at 37 °C in 5% CO_2 overnight with 1% v/v NucLight Red Lentivirus (Essen Bioscience, Cat.

No 4476). After replacement of the medium, different concentrations of the following reagents were then added to the wells: vehicle (DMSO), tubulysin, nigericin, and folate-nigericin. The plates were then placed in an IncuCyte S3 imaging instrument (Essen Bioscience), and each well was imaged every 4 h for 24 h using standard mode scan with a 10× objective and a red filter. Each assay concentration was replicated in three wells with five fields of view analyzed per well. Cell proliferation was quantified by counting the number of fluorescent nuclei over 24 h using the IncuCyte S3 Software (Essen Bioscience). Data was exported and analyzed using Graphpad Prism v 7. Cell growth is represented as percent confluence as a function of time. To determine the concentration that resulted in 50% growth inhibition (IC_{50}), the 24 h data points were graphed and normalized to vehicle treated control cells.

Confocal Microscopy of Ionophore-Treated Cells

Cells (100,000 cells/well in 0.5 mL culture medium) were seeded onto thin glass borosilicate Labtek 4-chambered dishes and incubated at 37 °C overnight to form a monolayer. On the following day, spent medium in each well was replaced with either fresh medium (well 1), fresh medium containing 10 nM folate-rhodamine conjugate **4** (well 2), or fresh medium containing either (i) folate-nigericin ester conjugate **2** (100 nM) and folate-rhodamine conjugate **4** (10 nM); or (ii) folate-nigericin amide conjugate **3** (100 nM) and folate-rhodamine conjugate **4** (10 nM); or (iii) folate-nigericin ester conjugate **2** (200 nM) and Dy647 labeled methylated folate-siRNA (400 nM); or (iv) folate carbamate nigericin conjugate **6** (30, 60, or 90 nM) and 10 nM folate-rhodamine conjugate **4**. Treated cells were incubated for 1 h at 37 °C before rinsing and replenishing with fresh medium (3 × 0.5 mL). The plated cells were then examined under an Olympus FV1000 Confocal Laser Scanning Microscope using a 60× oil-immersion objective over several hours (1–7 h) by excitation of either the rhodamine or Dylight 647 dyes. All fluorescence transmission images were obtained under identical conditions. The results section shows a representative sample out of all images collected.

Cell Lines and Culture

The FR-positive KB cell line was originally derived from a human nasopharyngeal epidermal carcinoma (33). KB cells used in this study had been maintained by the Cancer Cell Culture Facility in the Purdue University Department of Chemistry. It should be noted that KB cells purchased from the American Type Culture Collection are described as having the same origin but with the subsequent finding, based on isoenzyme analysis, HeLa marker chromosomes, and DNA fingerprinting, that they were actually established via HeLa cell contamination.[55] MDA-MB-231 cells were purchased from the American Type Culture Collection. MDA-MB-231 cells expressing high levels of FR were generated by passaging the cells for 14 weeks in folate-free cell culture medium. RAW264.7 cells is a murine macrophage-derived tumor cell line grown in folate-deficient medium.[56] The cell lines were cultured in folate-deficient FDRPMI 1640 medium (Invitrogen, Grand Island, NY) supplemented with 10% heat inactivated fetal bovine serum (Sigma-Aldrich, St. Louis, MO), penicillin (50 units/mL), and streptomycin (50 μg/mL) and passaged continuously in a monolayer at 37°C in a humidified atmosphere containing 5% CO_2.

Gene Knockdown Assay

The oligonucleotides were obtained from Integrated DNA Technologies, USA with the following modifications: siLuc2 sense/5Phos/rGrGrArCrGrAr-GrGrArCrGrArGrCrArCrUmUmCrUrU; siLuc2 antisense/ 5AzideN/ mGmArAmGrUrGmCrUmCrGmUrCmCrUm-CrGmUCCrUrU (m: 2-O-methyl bases r: RNA bases). For siRNA targeting assays, MDA-MB-231 cells were seeded in 6 well plates at a density of 1×10^6 cells/well and transfected with 2 μg of pmiRGlo plasmid (Promega) using Lipofectamine 2000 (Life Technologies). After 24 h, cells were reseeded into 96-well plates containing Fol-siLuc2, Fol-nigericin-siLuc2, Fol-NC (folate conjugated to nontargeting, negative control (NC) scrambled siRNA), Fol-nigericin-NC (folate conjugated to nontargeting, negative control (NC) scrambled siRNA) in folic acid, and serum free RPMI medium for a final concentration of 50 nM. Untreated and unconjugated duplex siRNA were also included as controls. For each time point, Renilla and firefly luciferase values were obtained using the Dual Luciferase Reporter kit (Promega) following the manufacturer's instructions. Firefly/Renilla ratios were normalized to Fol-NC or Fol-nigericin-NC for each time point. Experiments were performed three times with technical triplicates for each condition. Two-way analysis of variance (ANOVA) and Bonferroni post hoc test were used to test for statistical significance.

Supplementary Material

Refer to Web version on PubMed Central for supplementary material.

Acknowledgments

EC-119 (Pteroic acid-gGlu-Asp-Arg-Asp-Asp-Cys) was kindly donated by Endocyte, Inc. The folate-rhodamine conjugate **4** was donated by Dr. Sumith Kularatne (OnTarget Laboratories, LLC; Kurz Purdue Technology Center; 1281 Win Hentschel Blvd; West Lafayette, IN 47906). The Folate-siRNA-Dy647 conjugate was provided by Minnie Thomas, Department of Chemistry, Purdue University. The following shared resources of the Purdue University Center for Cancer Research (PCCR) were used to conduct the research reported in this paper: (1) Purdue University Interdepartmental NMR Facility; (2) Purdue University Flow Cytometry and Cell Sorting Facility. Funding for this research was provided by Endocyte Inc. Endocyte Inc.

We acknowledge Dr. Saif Hasan and Mr. Amar Parvate, Department of Biological Sciences, Purdue University for their help to measure the Cryo-TEM images of Liposomes used in this study.

ABBREVIATIONS

DCC	*N,N*-Dicyclohexylcarbodiimide
DMSO	Dimethyl sulfoxide
EC-119	(2*R*,5*S*,8*S*,11*S*,14*S*,19*S*)-19-(4-(((2-amino-4-oxo-3,4-dihydropteridin-6-yl)methyl)amino)benzamido)-5,8,14-tris-(carboxymethyl)-11-(3-guanidinopropyl)-2-(mercaptomethyl)-4,7,10,13,16-pentaoxo-3,6,9,12,15-pentaazaicosane-1,20-dioic acid
EtOAc	Ethyl acetate

FDRPMI	Folate-Deficient RPMI (Roswell Park Memorial Institute) Medium
FR	Folate receptor
LC-MS	Liquid chromatography–mass spectrometry
MeOH	Methanol
Proton sponge	Registered trademark for *N*,*N*,*N*′,*N*′-tetramethyl-1,8-naphthalenediamine
PyS-S-$(CH_2)_2$OH	2-(2-Pyridyldithio)-ethanol
RP-HPLC	Reversed-phase high-performance liquid chromatography
RT	Room temperature
TLC	Thin-layer chromatography

References

1. Smietana K, Siatkowski M, Møller M. Trends in clinical success rates. Nat Rev Drug Discovery. 2016; 15:379–380. [PubMed: 27199245]
2. Lightfoot HL, Hall J. Target mRNA inhibition by oligonucleotide drugs in man. Nucleic Acids Res. 2012; 40:10585–10595. [PubMed: 22989709]
3. Naldini L. Gene therapy returns to centre stage. Nature. 2015; 526:351–360. [PubMed: 26469046]
4. Tomlinson IM. Next-generation protein drugs. Nat Biotechnol. 2004; 22:521–522. [PubMed: 15122287]
5. Li G, Wang S, Xue X, Qu X, Liu H. Monoclonal antibody-related drugs for cancer therapy. Drug Discoveries Ther. 2013; 7:178–184.
6. Mahato RI, Narang AS, Thoma L, Miller DD. Emerging trends in oral delivery of peptide and protein drugs. Crit Rev Ther Drug Carrier Syst. 2003; 20:153–214. [PubMed: 14584523]
7. Zhang Y, Wang F. Carbohydrate drugs: current status and development prospect. Drug Discoveries Ther. 2015; 9:79–87.
8. Ernst B, Magnani JL. From carbohydrate leads to glycomimetic drugs. Nat Rev Drug Discovery. 2009; 8:661–677. [PubMed: 19629075]
9. Smaglo BG, Aldeghaither D, Weiner LM. The development of immunoconjugates for targeted cancer therapy. Nat Rev Clin Oncol. 2014; 11:637–648. [PubMed: 25265912]
10. Polakis P. Antibody Drug Conjugates for Cancer Therapy. Pharmacol Rev. 2016; 68:3–19. [PubMed: 26589413]
11. Govindan SV, Goldenberg DM. Designing immunoconjugates for cancer therapy. Expert Opin Biol Ther. 2012; 12:873–890. [PubMed: 22679911]
12. Twaites B, de las Heras Alarcón C, Alexander C. Synthetic polymers as drugs and therapeutics. J Mater Chem. 2005; 15:441–455.
13. Peeters M, Price T. Biologic therapies in the metastatic colorectal cancer treatment continuum – Applying current evidence to clinical practice. Cancer Treat Rev. 2012; 38:397–406. [PubMed: 21899955]
14. Rosman Z, Shoenfeld Y, Zandman-Goddard G. Biologic therapy for autoimmune diseases: an update. BMC Med. 2013; 11:88. [PubMed: 23557513]
15. Fessel WJ, Anderson B, Follansbee SE, Winters MA, Lewis ST, Weinheimer SP, Petropoulos CJ, Shafer RW. The efficacy of an anti-CD4 monoclonal antibody for HIV-1 treatment. Antiviral Res. 2011; 92:484–487. [PubMed: 22001594]

16. Zhang XQ, Sorensen M, Fung M, Schooley RT. Synergistic in vitro antiretroviral activity of a humanized monoclonal anti-CD4 antibody (TNX-355) and enfuvirtide (T-20). Antimicrob Agents Chemother. 2006; 50:2231–2233. [PubMed: 16723592]
17. Woo VC. A Review of the Clinical Efficacy and Safety of Insulin Degludec and Glargine 300 U/mL in the Treatment of Diabetes Mellitus. Clin Ther. 2017; 39:S12–S33. [PubMed: 28187863]
18. Yao S, Zhu Y, Chen L. Advances in targeting cell surface signalling molecules for immune modulation. Nat Rev Drug Discovery. 2013; 12:130–146. [PubMed: 23370250]
19. Koglin M, Hutchings C. Targeting G protein-coupled receptors with biologics for therapeutic use, Part 1. BioProcess Int. 2014; 12:38–45.
20. Lebwohl M, Tyring SK, Hamilton TK, Toth D, Glazer S, Tawfik NH, Walicke P, Dummer W, Wang X, Garovoy MR. A novel targeted T-cell modulator, efalizumab, for plaque psoriasis. N Engl J Med. 2003; 349:2004–2013. [PubMed: 14627785]
21. Martens E, Leyssen A, Van Aelst I, Fiten P, Piccard H, Hu J, Descamps FJ, Van den Steen PE, Proost P, Van Damme J. A monoclonal antibody inhibits gelatinase B/MMP-9 by selective binding to part of the catalytic domain and not to the fibronectin or zinc binding domains. Biochim Biophys Acta, Gen Subj. 2007; 1770:178–186.
22. Kaimal R, Aljumaily R, Tressel SL, Pradhan RV, Covic L, Kuliopulos A, Zarwan C, Kim YB, Sharifi S, Agarwal A. Selective blockade of matrix metalloprotease-14 with a monoclonal antibody abrogates invasion, angiogenesis, and tumor growth in ovarian cancer. Cancer Res. 2013; 73:2457–2467. [PubMed: 23423981]
23. Shete HK, Prabhu RH, Patravale VB. Endosomal escape: a bottleneck in intracellular delivery. J Nanosci Nanotechnol. 2014; 14:460–474. [PubMed: 24730275]
24. Doherty GJ, McMahon HT. Mechanisms of endocytosis. Annu Rev Biochem. 2009; 78:857–902. [PubMed: 19317650]
25. New EJ, Parker D. The mechanism of cell uptake for luminescent lanthanide optical probes: the role of macropinocytosis and the effect of enhanced membrane permeability on compartmentalisation. Org Biomol Chem. 2009; 7:851–855. [PubMed: 19225664]
26. McMahon HT, Boucrot E. Molecular mechanism and physiological functions of clathrin-mediated endocytosis. Nat Rev Mol Cell Biol. 2011; 12:517–533. [PubMed: 21779028]
27. Nabi IR, Le PU. Caveolae/raft-dependent endocytosis. J Cell Biol. 2003; 161:673–677. [PubMed: 12771123]
28. Varkouhi AK, Scholte M, Storm G, Haisma HJ. Endosomal escape pathways for delivery of biologicals. J Controlled Release. 2011; 151:220–228.
29. Erazo-Oliveras A, Muthukrishnan N, Baker R, Wang TY, Pellois JP. Improving the endosomal escape of cell-penetrating peptides and their cargos: strategies and challenges. Pharmaceuticals. 2012; 5:1177–1209. [PubMed: 24223492]
30. Behr JP. The proton sponge: a trick to enter cells the viruses did not exploit. CHIMIA Int J Chem. 1997; 51:34–36.
31. Selbo PK, Sandvig K, Kirveliene V, Berg K. Release of gelonin from endosomes and lysosomes to cytosol by photochemical internalization. Biochim Biophys Acta, Gen Subj. 2000; 1475:307–313.
32. Pasparakis G, Manouras T, Vamvakaki M, Argitis P. Harnessing photochemical internalization with dual degradable nanoparticles for combinatorial photo–chemotherapy. Nat Commun. 2014; 5:3623. [PubMed: 24710504]
33. Matsushita M, Noguchi H, Lu YF, Tomizawa K, Michiue H, Li ST, Hirose K, Bonner-Weir S, Matsui H. Photo-acceleration of protein release from endosome in the protein transduction system. FEBS Lett. 2004; 572:221–226. [PubMed: 15304352]
34. Terry J. The major electrolytes: sodium, potassium, and chloride. J Intraven Nurs. 1993; 17:240–247.
35. Scott CC, Gruenberg J. Ion flux and the function of endosomes and lysosomes: pH is just the start. BioEssays. 2011; 33:103–110. [PubMed: 21140470]
36. Harold F, Altendorf K, Hirata H. Probing membrane transport mechanisms with ionophores. Ann N Y Acad Sci. 1974; 235:149–160. [PubMed: 4527943]

37. Graven SN, Estrada-O S, Lardy HA. Alkali metal cation release and respiratory inhibition induced by nigericin in rat liver mitochondria. Proc Natl Acad Sci U S A. 1966; 56:654–658. [PubMed: 5229984]
38. Sturz GR, Phan THT, Mummalaneni S, Ren Z, DeSimone JA, Lyall V. The K+-H+ exchanger, nigericin, modulates taste cell pH and chorda tympani taste nerve responses to acidic stimuli. Chem Senses. 2011; 36:375–388. [PubMed: 21257734]
39. Yang J, Chen H, Vlahov IR, Cheng JX, Low PS. Evaluation of disulfide reduction during receptor-mediated endocytosis by using FRET imaging. Proc Natl Acad Sci U S A. 2006; 103:13872–13877. [PubMed: 16950881]
40. Vlahov IR, Leamon CP. Engineering folate–drug conjugates to target cancer: from chemistry to clinic. Bioconjugate Chem. 2012; 23:1357–1369.
41. Lee RJ, Wang S, Turk MJ, Low PS. The effects of pH and intraliposomal buffer strength on the rate of liposome content release and intracellular drug delivery. Biosci Rep. 1998; 18:69–78. [PubMed: 9743475]
42. Sabharanjak S, Mayor S. Folate receptor endocytosis and trafficking. Adv Drug Delivery Rev. 2004; 56:1099–1109.
43. http://sitem.herts.ac.uk/aeru/vsdb/Reports/2572.htm.
44. Xia W, Hilgenbrink AR, Matteson EL, Lockwood MB, Cheng JX, Low PS. A functional folate receptor is induced during macrophage activation and can be used to target drugs to activated macrophages. Blood. 2008; 113:438–446. [PubMed: 18952896]
45. Low PS, Kularatne SA. Folate-targeted therapeutic and imaging agents for cancer. Curr Opin Chem Biol. 2009; 13:256–262. [PubMed: 19419901]
46. Kalli KR, Oberg AL, Keeney GL, Christianson TJ, Low PS, Knutson KL, Hartmann LC. Folate receptor alpha as a tumor target in epithelial ovarian cancer. Gynecol Oncol. 2008; 108:619–626. [PubMed: 18222534]
47. Xia W, Low PS. Folate-targeted therapies for cancer. J Med Chem. 2010; 53:6811–6824. [PubMed: 20666486]
48. Srinivasarao M, Galliford CV, Low PS. Principles in the design of ligand-targeted cancer therapeutics and imaging agents. Nat Rev Drug Discovery. 2015; 14:203–219. [PubMed: 25698644]
49. Hilgenbrink AR, Low PS. Folate Receptor-Mediated Drug Targeting: From Therapeutics to Diagnostics. J Pharm Sci. 2005; 94:2135–2146. [PubMed: 16136558]
50. Leamon CP, Reddy JA. Folate-targeted chemotherapy. Adv Drug Delivery Rev. 2004; 56:1127–1141.
51. Zhao X, Li H, Lee RJ. Targeted drug delivery via folate receptors. Expert Opin Drug Delivery. 2008; 5:309–319.
52. Sudimack J, Lee RJ. Targeted drug delivery via the folate receptor. Adv Drug Delivery Rev. 2000; 41:147–162.
53. Lu Y, Low PS. Folate-mediated delivery of macromolecular anticancer therapeutic agents. Adv Drug Delivery Rev. 2002; 54:675–693.
54. Test procedures and acceptance criteria for new drug substances and new drug products: Chemical substances. International Conference on Harmonisation; Geneva: IFPMA; 1999.
55. Masters JRW. Human cancer cell lines: fact and fantasy. Nat Rev Mol Cell Biol. 2000; 1:233–236. [PubMed: 11252900]
56. Lu Y, Stinnette TW, Westrick E, Klein PJ, Gehrke MA, Cross VA, Vlahov IR, Low PS, Leamon CP. Treatment of experimental adjuvant arthritis with a novel folate receptor-targeted folic acid-aminopterin conjugate. Arthritis Res Ther. 2011; 13:R56–R56. [PubMed: 21463515]

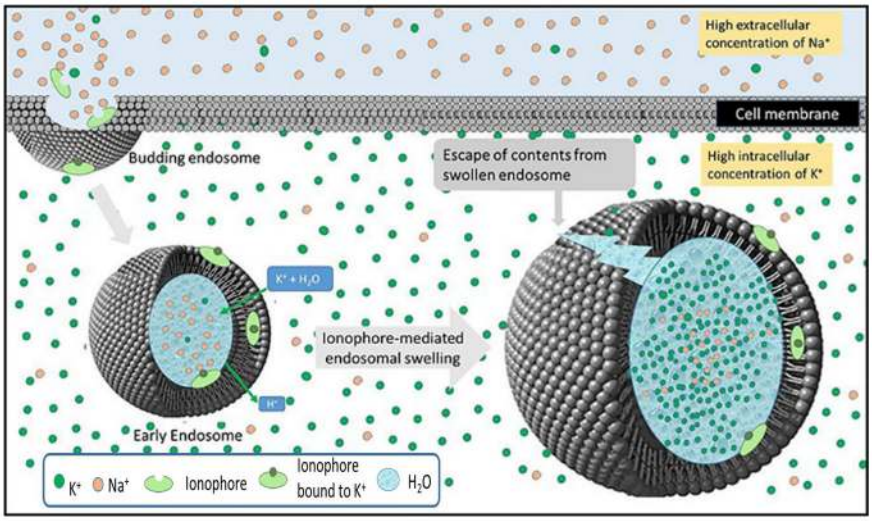

Figure 1.

Release of biologics from endosomal compartments using a K^+/H^+ ionophore to promote osmotic lysis of the endosomes. Endocytosis of a biologic into a target cell occurs by membrane invagination and budding as shown in the upper left corner. The lumen of the nascent early endosome will contain extracellular fluid characterized by high Na^+ concentration (orange spheres), while the cytosol surrounding the internalized endosome contains the usual high intracellular K^+ concentration (green spheres; left endosome). Codelivery of nigericin, an ionophore that transports K^+ in exchange for H^+, with a desired biologic into the endosome can then allow the electroneutral influx of K^+ in exchange for an eflux of H^+. Because K^+ is osmotically active while H^+ is not, this exchange results in endosome swelling (right endosome) and eventual lysis, releasing the biologic into the cell's cytosol. In the studies described below, nigericin is delivered together with a model biologic into the endosome by folate receptor-mediated endocytosis.

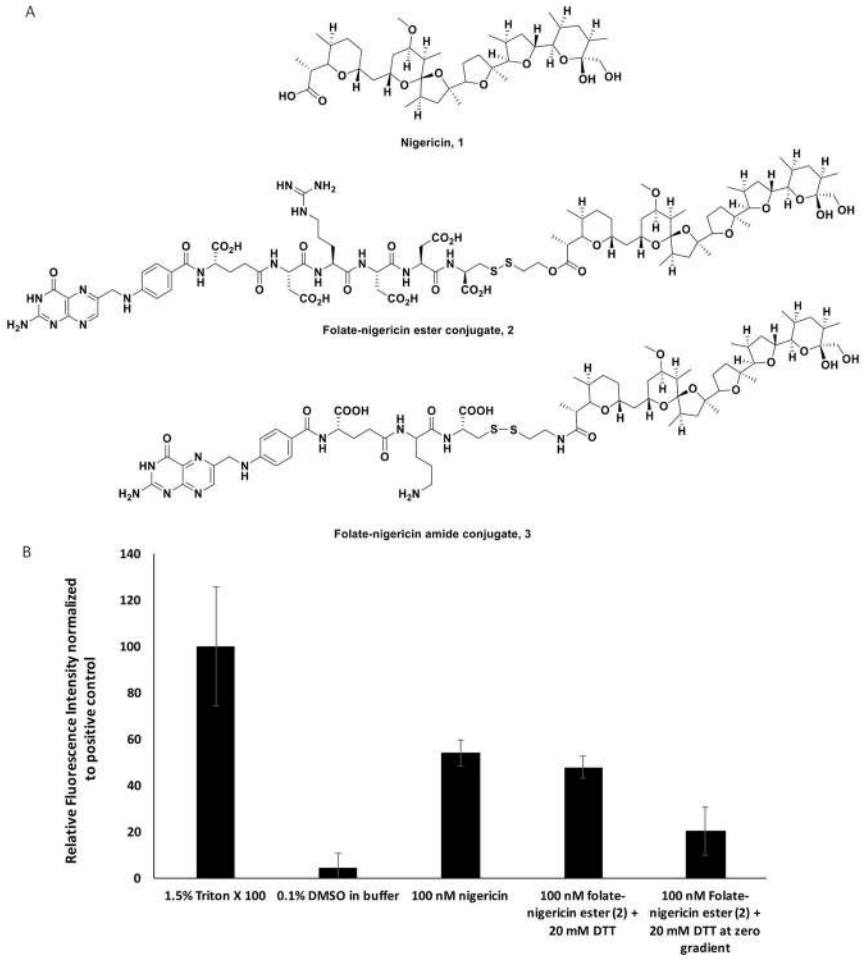

Figure 2.

Nigericin-mediated release of a membrane-impermeable calcein dye from unilamellar phospholipid vesicles. (A) Structure of nigericin, **1**, and folate-nigericin conjugates, **2** and **3**. (B) Bar graph quantitating the release of calcein from synthetic unilamellar vesicles prepared in 20 mM potassium phosphate buffer pH 7.0 containing 130 mM intralumenal NaCl and 130 mM extralumenal KCl, followed by incubation for 4 h in (i) 1.5% Triton X-100 (detergent) to release all intravesicular calcein; (ii) 0.1% DMSO in 130 mM KCl/20 mM K_3PO_4 buffer; (iii) 100 nM nigericin **1** dissolved in the same DMSO-containing buffer; (iv) 100 nM folate-nigericin ester conjugate **2** dissolved in the same buffer containing 20 mM dithiothreitol (DTT) to reduce the disulfide bond. As a second negative control, analogous liposomes were prepared with no Na^+ or K^+ gradient across their membranes (i.e., 130 mM KCl both inside and outside the liposome), and then treated with 100 nM folate-nigericin ester conjugate **2** dissolved in the same buffer containing 20 mM dithiothreitol (DTT) to reduce the disulfide bridge.

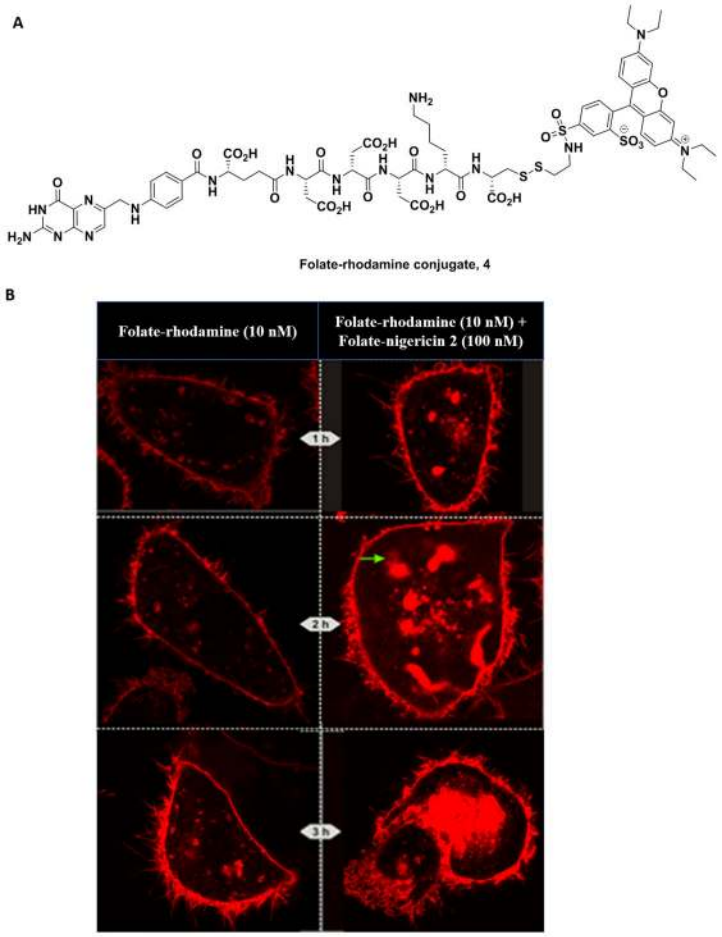

Figure 3.

Nigericin-mediated release of rhodamine entrapped in KB cell endosomes following folate receptor-mediated endocytosis. (A) Structure of the folate-rhodamine conjugate **4**. (B) Confocal fluorescence microscopy images of KB cells at 1 h (top), 2 h (middle), and 3 h (bottom) following treatment with 10 nM folate-rhodamine conjugate **4** either in the absence (left panels) or presence (right panels) of 100 nM folate-nigericin conjugate **2**. The green arrow at 2 h (middle panels) shows an example of the “pluming” phenomenon that we associate with escape of the dye from an entrapping endosome. By 3 h post-treatment, some of the swollen endosomes had merged into much larger compartments such as the one shown in the lower right-hand panel.

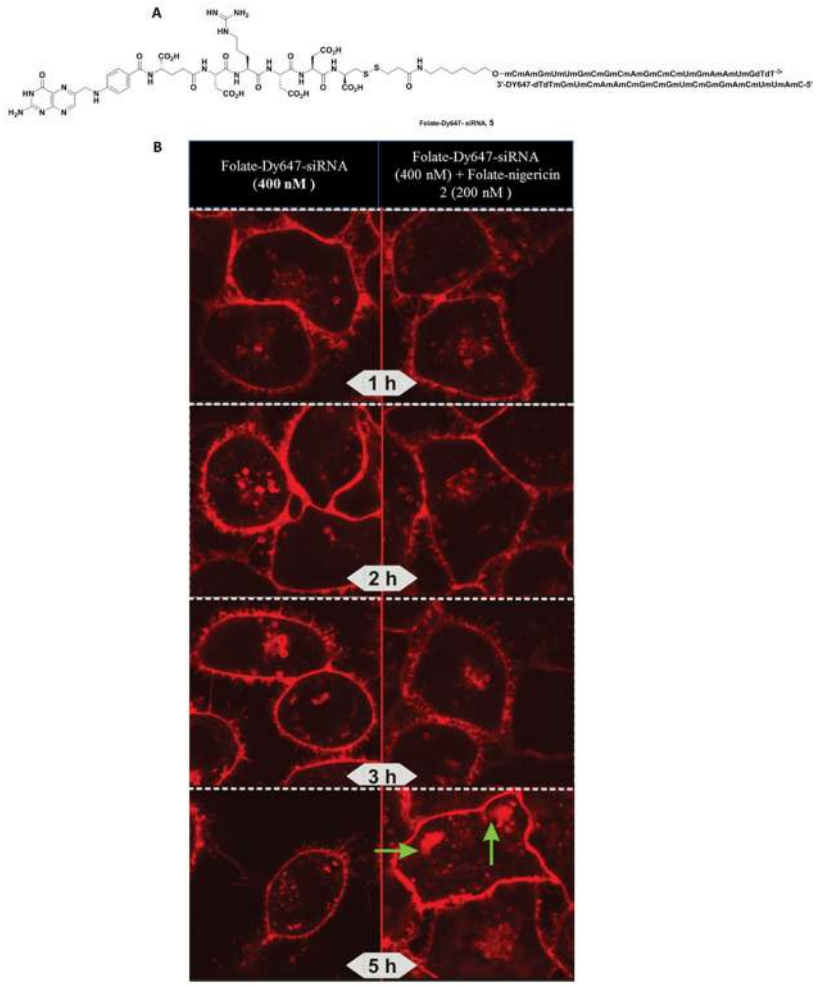

Figure 4.

Nigericin-mediated release of folate-Dy647-siRNA conjugate 5 from endosomes. (A) Structure of folate-Dy647-siRNA, **5**. (B) Confocal fluorescence microscopy images showing the release of Dy647-labeled folate-siRNA (400 nM) from endosomes of KB cells in the absence (left panels) and presence (right panels) of folate-nigericin conjugate **2**. The green arrows suggest “pluming” of contents as they stream away from the endosome.

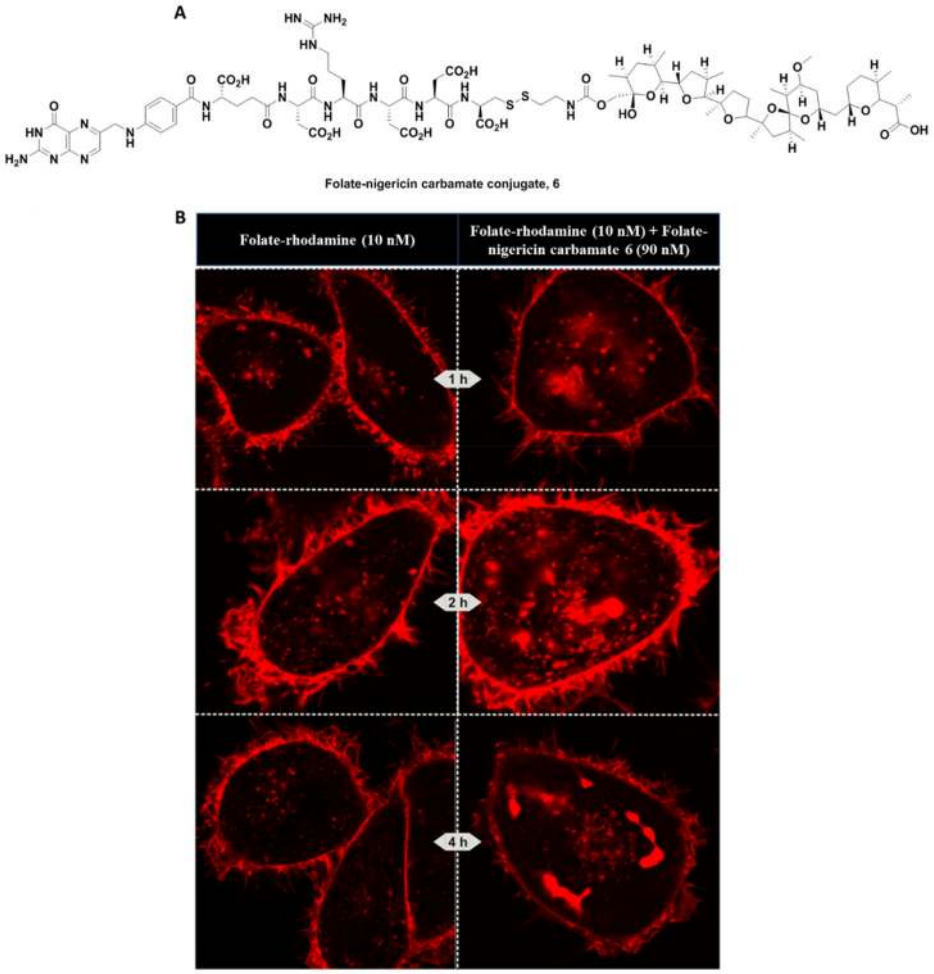

Figure 5.

Endosome release of folate-rhodamine **4** using carbamate functionalized folate-nigericin conjugate **6**. (A) Structure of folate-nigericin carbamate **6**. (B) Chronology of endosome swelling and folate-rhodamine escape over the first 4 h is shown for KB cells treated with 10 nM folate rhodamine conjugate **4** and 90 nM folate-nigericin carbamate conjugate **6**.

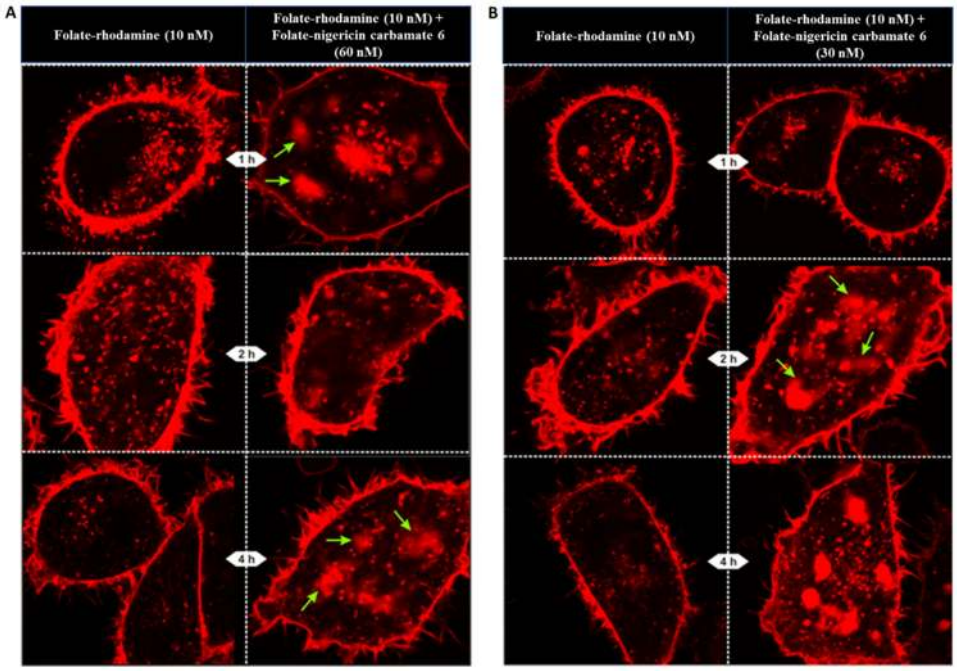

Figure 6.

Effect of lower concentrations of folate-nigericin carbamate **6** on escape of folate-rhodamine conjugate **4** from encapsulating endosomes. Endosome escape of 10 nM folate-rhodamine conjugate **4** from KB cells upon coadministration of either 60 nM (A) or 30 nM (B) of folate-nigericin carbamate conjugate **6** at the indicated times. Green arrows indicate examples of the pluming of endosomal contents.

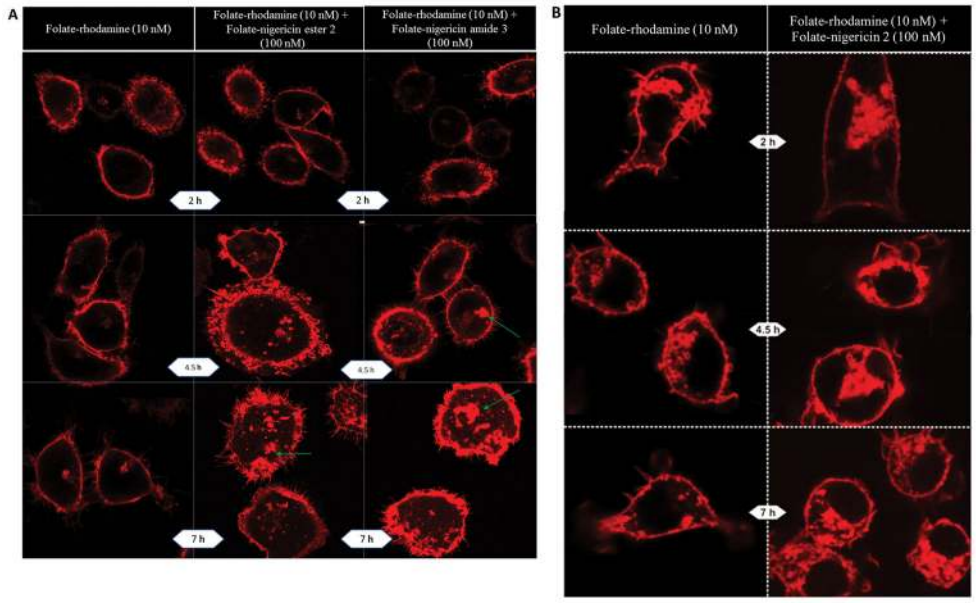

Figure 7.

Nigericin-mediated escape of rhodamine from endosomes in FRα-expressing MDA-MB-231 cells and FRβ-expressing RAW264.7 cells. (A) MDA-MB-231 cells were treated with 10 nM folate rhodamine conjugate **4** in the absence (left panels) or presence of 100 nM folate-nigericin ester conjugate **2** (middle panels) or 100 nM folate-nigericin amide conjugate **3** (right panels). The green arrows identify sites of "pluming" of contents as entrapped rhodamine streams away from the endosome. (B) Nigericin-mediated escape of rhodamine from endosomes in FRβ-expressing RAW264.7 cells. Cells were treated with 10 nM folate rhodamine conjugate **4** in the absence (left panels) or presence (right panels) of 100 nM folate-nigericin ester conjugate **2**.

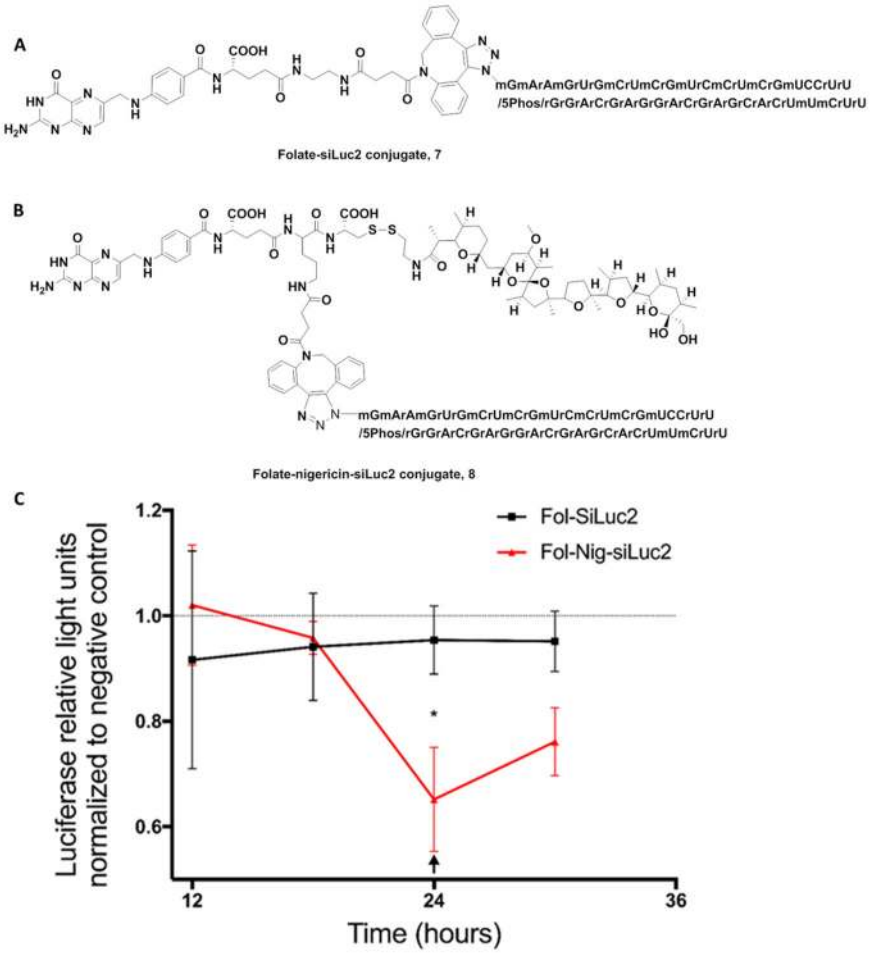

Figure 8.

Nigericin-mediated release of Folate-conjugated siLuc2. (A) Structure of Fol-siLuc2 **7**. (B) Structure of Fol-nigericin-siLuc2 conjugate **8**. (C) Luciferace2 enzyme activity in MDA-MB-231 cells as a function of time after treatment with either folate-siLuc2 or folate-nigericin-siLuc2 conjugate. Luciferase activity levels were normalized to a negative control (a scrambled siRNA). Mean ± S.D., technical replicates = 3, $n = 3$, * $P < 0.05$. The arrow indicates replacement of media with a new dose of folate conjugates (50 nM). Fol-SiLuc2: Folate-siLuc2; Fol-Nig-SiLuc2 conjugate: Folate-nigericin-siLuc2 conjugate. The gene-knockdown experiment indicated a rapid reduction in luciferase activity in Fol-nigericn-siLuc2 treated cells as soon as 18 h post treatment and reaches 30–35% after 24 h.